KSCE Journal of Civil Engineering (2018) 22(4):1304-1315

DOI 10.1007/s12205-017-1321-3

Structural Engineering

pISSN 1226-7988, eISSN 1976-3808
www.springer.com/12205

Investigation of the LS Level Hysteretic Damping Capacity of Steel MR Frames' Needs for the Direct Displacement-Based Design Method

Reza Esmaeil Abadi* and Omid Bahar**

Received August 14, 2016/Revised March 12, 2017/Accepted May 11, 2017/Published Online August 1, 2017

Abstract

Proper modeling of the Hysteretic Damping (HD) capacity of structural models at a desired performance level is the key requirement for reliable estimation of design base shears in Direct Displacement-based Design (DDBD) method. Priestley and his colleagues on the basis of their research, have proposed a formula to predict the HD capacity of Steel Moment-resisting Frames (SMRFs) which is presented in DBD12. The current study examined this relation and proposes a reliable equation for design of SMRFs using DDBD method at the Life Safety (LS) performance level and the Equivalent Viscous Damping (EVD) hypothesis. For this purpose, a wide range of SMRFs were analysed using linear/nonlinear static/dynamic time history methods under different loading conditions. The damping ratios of all models were calculated using Jacobsen's and Jennings's formulas and the procedure proposed by FEMA-440. The results show an exponential trend that diverges from the empirical formula presented in DBD12. Two new relations are proposed for hysteretic damping based on ductility and the ratios of the initial and equivalent periods.

Keywords: *direct displacement-based design, equivalent viscous damping, nonlinear static analysis, equivalent period, sinusoidal loading protocol*

1. Introduction

The direct displacement-based design (DDBD) method was first introduced by Priestly (1993) and has been widely studied in Europe, New Zealand and North America. In DDBD method structures must be designed for a specific performance level. This performance level can be defined by setting drift limits associated with specific ground motion risk levels. DDBD is a step-by-step method for determination of the limiting forces for structural members. A multi-degree-of-freedom (MDOF) structure is represented by an idealized single-degree-of-freedom (SDOF) substitute structure. This is defined by the characteristic design displacement, yield displacement, equivalent height and equivalent mass in this system (Cecilia *et al*., 2015). The necessary analysis and relations are then presented on the basis of the substitute structure.

The purpose of DDBD method is to preserve the simplicity and applicability of the analysis. The fundamental relations and principles used in DDBD method were initially developed and tested for reinforced concrete structures. After extensive research over the course of many years, these design regulations have been generalized to include steel structures. The DDBD method was first proposed as a substitute for the force-based design method (Priestley *et al*., 2007; Wijesundara *et al*., 2011) and was later developed to include many other types of structures (Blandon *et al*., 2005; Cecilia *et al*., 2015).

A major advantage of the simple substitute structure approach is its ability to obtain the inelastic characteristics of a multi-degree-of-freedom structure during an earthquake (Shibata *et al*., 1976). Moreover, unlike the force-based method which employs initial stiffness, in DDBD, the substitute structure characteristics are expressed through the secant stiffness at maximum displacement and equivalent damping (sum of elastic damping and hysteretic damping). This method later was suggested as a draft of direct displacement-based structural design and published in 2009 as DBD09 (Calvi *et al*., 2009). The latest revised edition of DDBD method was published in 2012 as DBD12 (Sullivan *et al*., 2012).

The aims of the current study were to employ the DDBD method to analyze the effect of the number of spans and stories of a moment frame on structural damping capacity and to compare the results with those obtained from the Priestley equation. The study employed this method to estimate the damping ratios of the moment frames using Equivalent Viscous Damping (EVD). For this purpose, in the second section of the paper, a closer look at equivalent viscous damping is conducted, and the significance of the research is demonstrated in section 3. The two-dimensional (2D) steel frames used are presented in section 4. Section 5 and 6 represent the analyses, findings and the

*Ph.D. Student, Dept. of Civil Engineering, Science and Research Branch, Islamic Azad University, Tehran, Iran (E-mail: Esmaeilabadi@riau.ac.ir)
**Assistant Professor, Structural Engineering Research Center, International Institute of Earthquake Engineering & Seismology (IIEES), Tehran, Iran (Corresponding Author, E-mail: omidbahar@iiees.ac.ir)

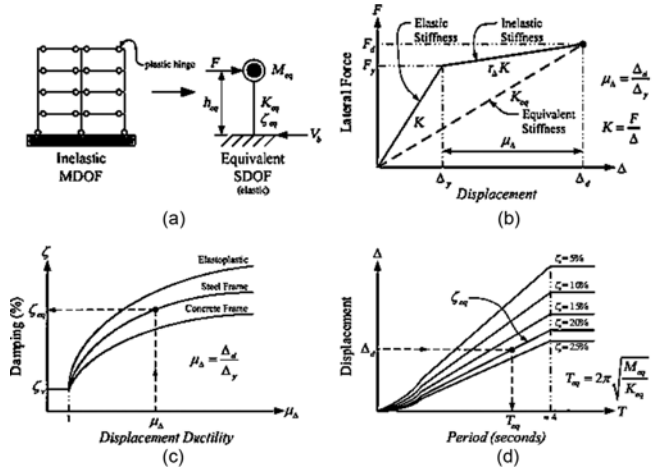

Fig. 1. Fundamentals of Direct Displacement-Based Design (Priestley *et al.*, 2007): (a) SDOF Simolation of Inelastic MDOF, (b) Idealized Force-Displacement of Equivalent SDOF, (c) Equivalent Viscous Damping vs Ductility, (d) Displacement Response Spectra

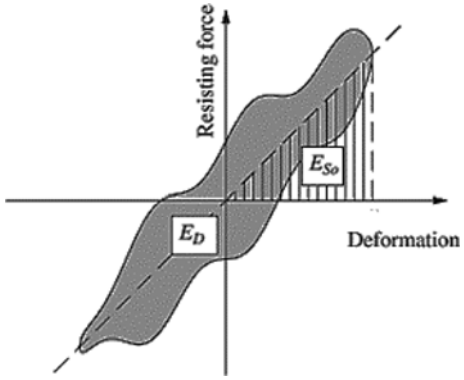

Fig. 2. Definition of Energy Dissipated E_D in One Cycle of Harmonic Vibration and Maximum Strain Energy E_{so} (Chopra, 2013)

evaluation of results. Section 7 presents the conclusions. A general review on the procedure of DDBD method is in the Appendix.

The fundamentals of the DDBD method are shown in Fig. 1. Fig. 1(a) represents the building with a single degree of freedom (SDOF) model and Fig. 1(b) builds a bilinear relationship between lateral force and displacement. DDBD method uses secant stiffness k_{eq} to represent structural stiffness during inelasticity at target displacement Δ_d. Fig. 1(c) finds Equivalent Viscous Damping (EVD) ζ_{eq} for a given level of ductility demand. The equivalent period is obtained, as shown in Fig. 1(d).

The design steps and formulas used in DDBD method for steel moment-resisting frames are given in the Appendix (Sullivan *et al.*, 2012).

2. Equivalent Viscous Damping

Proper estimation of the Hysteretic Damping (HD) capacity of structural models at a desired performance level is the key to DDBD method and ensure estimation of reliable design base shear. Priestley and his colleagues, on the basis of their research into concrete buildings, have proposed a formula to predict the HD capacity of steel moment-resisting frames (SMRFs), as presented in DBD12. Previous evaluations performed on steel structures designed using DBD12, including moment frames, have shown that the nonlinear responses of these steel frames are less than the values expected in the primary design process (Esmaeilabadi, 2016). The majority of this difference relates to the empirical relations used for estimation of HD. In 1930 Jacobsen was the first to propose equivalent linearization by use of an elastic SDOF system instead of a damped nonlinear system (Dwairi, 2004). In 1968 Jennings further argued that the natural frequency of a nonlinear system would decrease as a result of yielding, whereas no such observation had been reported in the Jacobsen problem (Dwairi *et al.*, 2007). Jennings proposed that the equivalent SDOF system had to exhibit different resonance frequencies at different damping ratios and concluded that the equivalent damping method was an exact definition of steady-state response under sinusoidal excitation. According to his studies, equivalent damping can be obtained from Eq. (1) (Chopra, 2013) as:

$$\zeta_{eq} = \frac{1}{4\pi}\frac{1}{\frac{\omega}{\omega_n}}\frac{E_D}{E_{S0}} \tag{1}$$

where E_D is the energy dissipated by viscous damping in one cycle of harmonic vibration, E_{so} is the maximum strain energy (Fig. 2), ω_n is the natural frequency and ω is the excitation frequency.

3. Significance of the Research

In the ultimate strength design method, displacement and deflection contribute to the instability of the structure, and exacerbate the structure's condition. It is imperative to incorporate a new method which is capable of considering displacement at the outset of design. Several studies were carried out in parallel and formulations were proposed for the analysis of steel structures; however, evaluations indicate that such formulations are of poor accuracy and limited application in practice, increasing the need for accurate new design methods.

The displacement of a structure is relevant to its performance, and correlates with deflections, makes displacement a significant issue at the design stage. DDBD is a recent performance-based design method which has proven to be proper for solving such problems at the design stage. Despite its precision for the design of concrete structures, DDBD has not been employed for steel structures. The reliability and accuracy of this method mainly depends on the proper estimation of EVD, and where any deviation in EVD is likely to divert analysis into disastrous calculations of the forces and base shear.

It is of great importance to model hysteretic damping based on EVD. Because improper calculation of the elastic spectrum can

introduce error into the direct displacement method, the present study adopted structural code design spectra to construct elastic displacement spectra at different damping ratios for use in SeismoSignal (2015). The frames studied were designed according to the requirements of the Iranian Code of Practice for Seismic Resistant Design of Buildings (Standard No. 2800, 2014) which is mostly the same as ASCE (2010). Investigation of 3 up to 15-story structures and analyses of pushover, modal, dynamic, sinusoidal loading and static time history broadens the scope of the study and contributes to the validity and applicability of the results.

4. 2D Frames used in this Study

In this study, 30 moment-resisting frames having different number of stories (3, 6, 9, 12, and 15) and different bays (3 and 6 bays) were studied. A general view of the 2D frames is shown in Fig. 3. The sections were designed according to the INBCSD (2013) which is mostly the same as AISC (2010). The seismic forces were extracted from the Iranian code of practice for

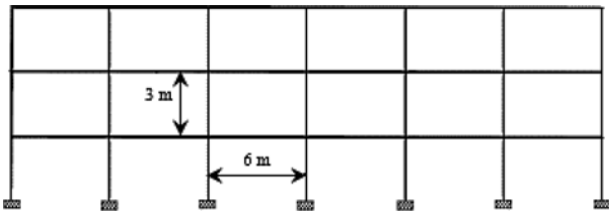

Fig. 3. General View of the Designed Frames

Table 1. The Properties of Materials and Design Parameters

Specifications		Value	Unit
Steel density	P_s	7795	kg/m^3
Steel modulus of elasticity	E_s	2.1×10^{10}	kg/m^2
Poisson's ratio	υ	0.3	
Yield strength of steel	F_y	2.4×10^{7}	kg/m^2
Ultimate strength of steel	F_u	3.7×10^{7}	kg/m^2
Directional symmetry type		Isotropic	
Type of hysteresis		Kinematic	
Soil type for the structure site		Type III-Class D	
Dead load applied to the frame		2400	kg/m
Live load applied to the frame		800	kg/m

Table 2. Details of Frames Designed in this Study

Data				Sections
Name	n_b	n_s	P_i	Column-Beam (Story)
3-3-P_a	3	3	0.259	240-330(1)+240-270(2-3)
3-3- P_b	3	3	0.196	260-330(1)+260-270(2-3)
3-3- P_c	3	3	0.19	280-330(1)+280-330(2)+280-270(3)
3-6- P_a	6	3	0.296	240-330(1)+240-270(2-3)
3-6-P_b	6	3	0.224	260-330(1)+260-270(2-3)
3-6-P_c	6	3	0.217	280-330(1)+280-330(2)+280-270(3)
6-3- P_a	3	6	0.25	280-360(1)+280-360(2-3)+280-300(4)+260-300(5)+260-270(6)
6-3-P_b	3	6	0.192	300-360(1)+300-360(2-3)+300-300(4)+280-300(5)+280-270(6)
6-3-P_c	3	6	0.188	320-360(1)+320-360(2-3-4)+300-330(5)+300-270(6)
6-6- P_a	6	6	0.313	280-360(1)+280-360(2-3)+280-300(4-5)+260-270(6)
6-6-P_b	6	6	0.241	300-360(1)+300-360(2-3)+300-300(4)+280-300(5)+280-270(6)
6-6-P_c	6	6	0.215	320-360(1)+320-360(2-3-4)+300-330(5)+300-270(6)
9-3- P_a	3	9	0.187	340-360(1)+340-400(2-3-4-5)+320-360(6)+320-300(7)+300-300(8)+300-270(9)
9-3-P_b	3	9	0.158	360-360(1)+360-400(2-3-4-5)+340-360(6)+340-300(7)+320-300(8)+320-270(9)
9-3-P_c	3	9	0.133	400-360(1)+400-400(2-3-4-5)+360-360(6-7)+320-330(8)+320-270(9)
9-6- P_a	6	9	0.213	340-360(1)+340-400(2-3-4-5)+320-360(6)+320-300(7)+300-300(8)+300-270(9)
9-6-P_b	6	9	0.18	360-360(1)+360-400(2-3-4-5)+340-360(6)+340-300(7)+320-300(8)+320-270(9)
9-6-P_c	6	9	0.152	400-360(1)+400-400(2-3-4-5)+360-360(6-7)+320-330(8)+320-270(9)
12-3- P_a	3	12	0.15	400-360(1)+400-400(2-3)+400-450(4-5)+360-400(6-7)+340-330(8-9-10)+340-270(11-12)
12-3-P_b	3	12	0.125	450-360(1)+450-400(2-3-4-5)+400-450(6-7)+360-330(8-9-10)+360-270(11-12)
12-3-P_c	3	12	0.093	500-360(1)+500-400(2-3)+500-450(4-5)+450-450(6-7)+400-400(8-9)+400-360(10)+400-270(11-12)
12-6- P_a	6	12	0.171	400-360(1)+400-400(2-3)+400-450(4-5)+360-400(6-7)+340-330(8-9-10)+340-270(11-12)
12-6-P_b	6	12	0.143	450-360(1)+450-400(2-3)+450-450(4-5)+400-450(6-7)+360-330(8-9-10)+360-270(11-12)
12-6-P_c	6	12	0.106	500-360(1)+500-400(2-3)+500-450(4-5)+450-450(6-7)+400-400(8-9)+400-360(10)+400-270(11-12)
15-3- P_a	3	15	0.078	500-300(1)+500-400(2-3)+500-450(4-5)+450-400(6-7)+400-400(8-9)+400-360(10)+400-330(11-12-13-14-15)
15-3-P_b	3	15	0.059	550-300(1)+550-400(2-3)+550-450(4-5)+500-400(6-7)+450-400(8-9)+450-360(10)+450-330(11-12-13)+450-300(14-15)
15-3-P_c	3	15	0.068	600-300(1)+600-400(2-3)+600-450(4-5)+550-450(6-7)+500-450(8-9)+500-400(10)+500-330(11-12-13)+500-300(14-15)
15-6- P_a	6	15	0.09	500-300(1)+500-400(2-3)+500-450(4-5)+450-400(6-7)+400-400(8-9)+400-360(10)+400-330(11-13-13)+400-300(14-15)
15-6-P_b	6	15	0.067	550-300(1)+550-400(2-3)+550-450(4-5)+500-400(6-7)+450-400(8-9)+450-360(10)+450-330(11)+450-330(12-13-14)+450-330(15)
15-6-P_c	6	15	0.077	600-300(1)+600-400(2-3)+600-450(4-5)+550-450(6-7)+500-450(8-9)+500-400(10)+500-330(11)+500-330(12-13-14-15)

seismic resistant design of buildings (Standard No. 2800, 2014). The properties of the materials and design parameters are presented in Table 1.

Table 2 lists the sections designed for the frames under study. In this table, the naming convention of the frames employs two numbers and P_i parameter. The two numbers represent the number of stories (n_s), and the number of frame bays (n_b), respectively, and P_i can be obtained in Eq. (2) (Dimopoulos *et al*., 2012) as:

$$P_i = \frac{\sum\left(\frac{I}{L}\right)beam}{\sum\left(\frac{I}{L}\right)column} \qquad i = a, b, c \tag{2}$$

where, I and L denote the inertia moment and length of beam or column, respectively.

According to the design code, $P_i < 0.5$ should be used to assure the maximum structural capacity during strong earthquakes. In this study in order to investigate the effect of ductility, for each number of story and bay, three different size of column were used that caused three different values of P_i refers as P_a, P_b and P_c ($P_a > P_b > P_c$). For example according to the Table 2 the case of 3-6- P_a indicates a 3 story and 6 bay structure having the value of P_a equal to 0.259. The size of IPB and IPE sections used for the given stories for columns and beams, respectively, are provided in Table 2. For instance, "240-330(1)+240-270(2-3)" denotes IPB240 columns and IPE330 beams are used in the first story while the 2nd and 3rd stories employ IPB240 and IPE270 sections as column and beam, respectively.

5. Analysis of Frames in Order to Obtaining the Equivalent Viscous Damping

To achieve the objectives of this study, different types of analysis were conducted on the frames. Some different kinds of software and analysis methods were used to verify the designed models and minimize the possible modeling error. Table 3 lists the material properties and nonlinear characteristics used in each kinds of software and analysis methods according to FEMA 356 (2000). It is mentioned the plastic hinges form at first and end of beams and columns. The damping ratio calculated for the frames was assumed to be equal to the hysteretic damping ratio. In addition, the elastic damping ratio was disregarded in the calculations as illustrated in the Appendix. In nonlinear analyses the Hilber-Hughes-Taylor method was used in all kinds of software. Due to large volume of calculation, tables and figures for all studied frames, only the results for frame 6-3- P_a were presented as sample in section 5.1 up to 5.8. It is noted the methods used for the other frames are the same as frame 6-3- P_a. The results for all frames were demonstrated in section 6.

5.1 Specifications of the Equivalent Structure using DDBD Method

Table 4 shows the specifications of the equivalent structure obtained by Eqs. (6) to (17) and assuming $\theta_c = 0.02$ from DDBD method for frame 6-3- P_a. These results were subsequently compared with those obtained from numerical analysis. Parameters θ_c, Δ_d, M_{eq}, h_{eq}, Δ_y, μ_Δ and ξ_{hyst} are given in the Appendix.

5.2 Modal Analysis

The results of the modal analysis for the 6-3- P_a frame are presented in Table 5. A comparison of the initial (natural) periods and shape of first mode reveals that the respective models were proper. The shape of first mode of the frame was used as the modal load pattern in nonlinear static analysis, and the period was used in sinusoidal time history analysis.

5.3 Nonlinear Static Analysis (Pushover)

Table 6 shows the results obtained for the 6-3- P_a frame from nonlinear static analysis in SAP2000. The corresponding values

Table 3. The Modeling Parameters and Analysis Types used in Each Kinds of Software

Software	Material Type	Nonlinear Properties	Analysis
SAP2000	Bilinear steel model	Concentrated hinge, according to FEMA 356 M3 for beams and P-M3 for columns	Modal - pushover
Abaqus	Bilinear steel model	Wire Elements	Modal - pushover – Dynamic time history- Static time history
SeismoStruct	Bilinear steel model	Fiber Elements	Modal - pushover – Dynamic time history- Static time history
OpenSees	Steel02	Nonlinear-Beam-Column Fiber Elements	Modal – pushover- Dynamic time history- Static time history

Table 4. Specifications the Equivalent Structure using DDBD Method

Frame	Parameter	Δ_d(m)	M_{eq}(Kg)	h_{eq}(m)	Δ_y(m)	μ_Δ	ξ_{hyst}
	Equation	(10)	(11)	(12)	(15)	(13)	(16), (17)
6-3- P_a		0.26	195383.75	12.66	0.14	1.94	9

Table 5. Results of Modal Analysis in Different Kinds of Software

Story	Shape of first mode			Seismic weight (kg)	The initial period (s) (T_i)			
	OpenSees	SeismoStruct	SAP2000		Sap2000	Abaqus	OpenSees	SeismoStruct
6	1	1	1	230400	1.15	1.16	1.12	1.12
5	0.9	0.9	0.9					
4	0.75	0.75	0.76					
3	0.56	0.57	0.57					
2	0.35	0.36	0.36					
1	0.13	0.14	0.15					

Table 6. Results of Nonlinear Static Analysis in SAP2000

Load pattern analysis		FEMA-440		
load	Gravity load	T_{eq} (s)	Δ_d (m)	ζ_{hyst}
Uniform	0.9D	1.486	0.28	9%
	1.1D+0.275L	1.523	0.28	10%
Modal	0.9D	1.651	0.29	9.8%
	1.1D+0.275L	1.488	0.293	10.6%

for target displacement, equivalent period (see the Appendix) at the life-safety performance level (according to the Appendix, θ_c = 0.02), and the hysteretic damping ratio for the structure were obtained according to the definitions presented in FEMA-440 (2005). In performance based design method for a structure, the life safety performance level is the level that some residual strength and stiffness left in all stories, there is some permanent drift and structure may be beyond economical repair.

As the researchers had obtained different results for similar building, the FEMA-440 project was defined in 2005 to obtain converging results from these methods by achieving a simple and relatively exact method for nonlinear analysis of seismic performance of structures. In this study, the effects of higher modes as well as additional degrees of freedom were included.

Powell and Emeritus stated that, because the relations presented in FEMA-440 are defined on the basis of their ductility intervals, these should provide more reliable and exact results. For this reason, the hysteretic damping obtained from this source was used as the basis of calculations in this section (Powell *et al*., 2013).

5.3.1 Determining Yield Displacement using Pushover Analysis

The yield displacement of the frames was calculated using pushover analysis and the results for sample frame 6-3- P_a are shown in Fig. 4(a) using different kinds of software. The agreement between these results demonstrates the correctness of the structural modeling method. Yield displacement for the respective structural models was obtained by bilinearizing the diagrams as shown in Fig. 4(b). The yield displacement and final displacement results obtained from pushover analysis were 0.15 and 0.286 m, respectively.

5.4 Nonlinear Dynamic Time History Analysis Based on Accelerograms of Design Code

To further ensure the validity of the final displacement obtained by pushover analysis and to compare the results with that of the DDBD method, nonlinear dynamic time history analysis was conducted using seven artificial accelerograms. The artificial accelerograms of the design spectrum are adopted from the design code. These accelerograms were generated by SIMQKE (Gasparini *et al*., 1976), which simulates motions that can be used for more realistic earthquake-resistant design of structures. Their response spectra as well as mean values were compared with those of the design spectrum (Fig. 5).

All the accelerograms were equalized such that their acceleration response spectra could be matched with the Type III soil design spectrum in the design code. Because the frames were designed based on soil Type III, this matching was necessary to interpret the results in an acceptable way.

Soil Type III is the most general soil is designed structure

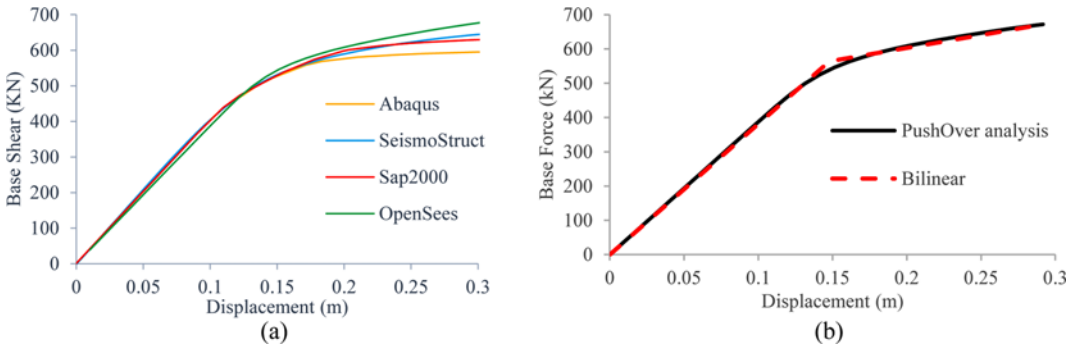

Fig. 4. (a) Pushover Curves Obtained from Different Kinds of Software, (b) Bilinearized Curve

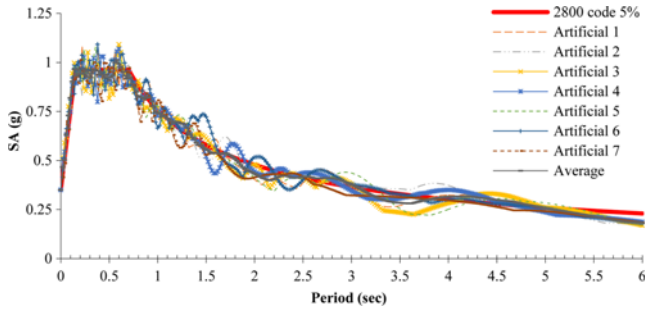

Fig. 5. Artificial Spectrum Records Used in the Analysis

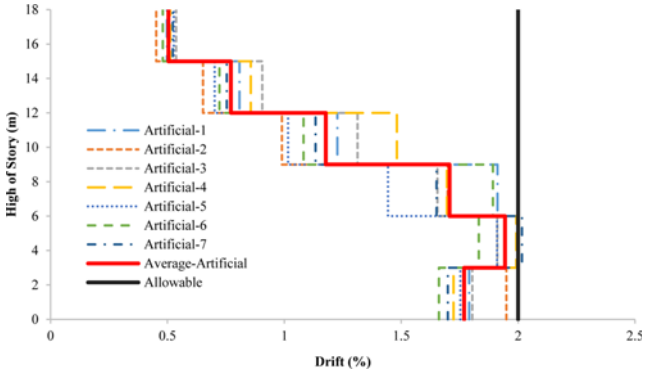

Fig. 6. Drift profile Applying Accelerograms for Sample Frame 6-3- P_a

Table 7. Target Displacement of Artificial Records for Frame 6-3- P_a

Artificial records	SeismoStruct	OpenSees
	Target Displacement (m)	Target Displacement (m)
Artificial-1	0.31	0.29
Artificial-2	0.28	0.29
Artificial-3	0.26	0.28
Artificial-4	0.32	0.26
Artificial-5	0.22	0.32
Artificial-6	0.29	0.31
Artificial-7	0.25	0.26
Average	0.27	0.28

which is the same as soil Class D in ASCE. This soil includes the stiff soil with 175 m/s $< \bar{v}_s \leq$ 375 m/s, where, $\bar{v}_s$ is the shear wave velocity.

Table 7 shows the target displacement results obtained for frame 6-3- P_a.

The drift profiles in the different records are compared in Fig. 6. Note that the drift profile obtained from all analyses was less than limit value of 2%.

5.5 Dynamic Time History Analysis Under Sinusoidal Loading

As described in section 2, to calculate the damping ratio, the hysteresis diagram of the moment frames under dynamic loading must be used. Because of the characteristics of accelerograms, no regular or desirable hysteresis loop could be obtained from such loads. The present study used regular harmonic loads based on the natural period of a structure; thus, sinusoidal loads with periods equal to the initial and equivalent periods of the structure calculated at the instant of the final displacement were prepared.

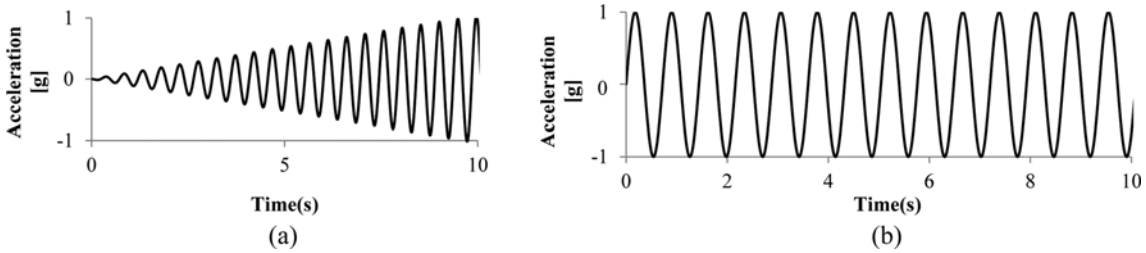

Fig. 7. Example of Sinusoidal Records Used in Present Study: (a) Increasing Sinusoidal, (b) Harmonic Sinusoidal Accelerograms

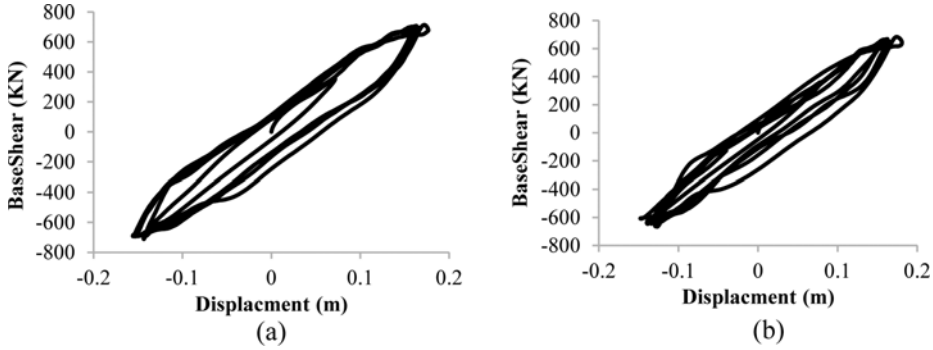

Fig. 8. Comparison of the Hysteresis Loops Obtained using Sinusoidal Records and Equivalent Period for Sample Frame 6-3- P_a: (a) OpenSees, (b) Abaqus

For example, the initial and equivalent periods for frame 6-3- P_a were, respectively, 1.14 and 1.53 s.

The initial period (T_i) and equivalent period (T_{eq}) were obtained from previous analyses (see sections 5.2 and 5.3). To obtain the maximum capacity of the frames, uniform, increasing and decreasing sinusoidal loading was applied. In each loading, the amplitude and number of vibratory cycles in the harmonic sinusoidal accelerograms were varied to evaluate the maximum capacity of the structure (i.e., formation of more plastic hinges). Fig. 7 is an example of the harmonic records used.

Figure 8 shows the hysteresis loop for sample frame 6-3- P_a, based on the results obtained from OpenSees and Abaqus under sinusoidal loading and equivalent periods. As seen, these loops are in good agreement.

Based on the time history analysis under sinusoidal loading at the initial and equivalent periods, a hysteresis loop was plotted and the damping ratio was calculated for different frames. The important point in these analyses is the comparison of damping ratios under the two different loading conditions. The initial period generated more number of plastic hinges in the structure, perhaps because of resonance, thus achieving higher damping ratios. In other words, structural resonance increased the response nonlinearity and thereby elevated the structural damping capacity.

5.6 SDOF Structural Analysis Under Sinusoidal Loading

The DDBD method substitutes an MDOF structure with an SDOF structure. It is known that the displacement spectrum can be defined only for SDOF systems. In order to obtaining the equivalent viscus damping the following method was used:

a. The maximum displacement of the frame 6-3- P_a using a sinusoidal record was obtained 18 cm according to Fig. 8.
b. The various displacement spectrums were drawn for the same sinusoidal record with different damping values as shown in Fig. 9.
c. Then the damping value (12%) which caused the maximum displacement equal to 18 cm was selected as the hysteretic damping of frame 6-3- P_a.

5.7 Static Time History Analysis

To produce more accurate results, static time history analysis with increasing sinusoidal protocol was used to determine the hysteresis loop to obtain the damping ratio in accordance with the explanations presented in section 2. The relevant protocol was based on static time history analysis adapted from the protocols introduced in ATC-40 (1996) as shown in Fig. 10. As explained in Section 2, with regard to the final point loading protocol, the final cycle in the static time history analysis is equal to the final displacement in each frame.

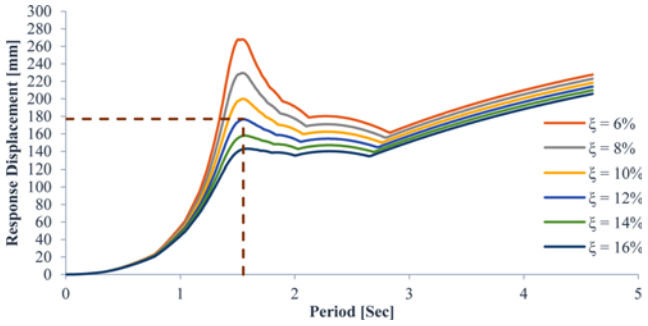

Fig. 9. Calculated Damping Ratio of a SDOF Structure for Frame 6-3- P_a

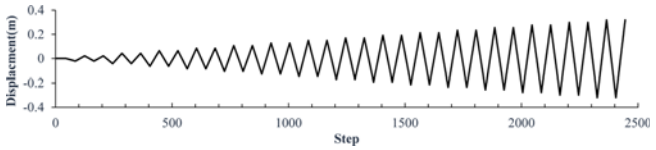

Fig. 10. Protocol of Nonlinear Static Time History Analysis for Frame 6-3- P_a

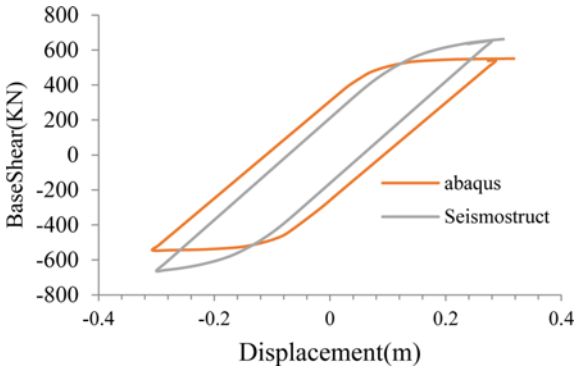

Fig. 11. Comparison of Hysteresis Loops in Static Time History Analysis for Frame 6-3- P_a

Table 8. Hysteretic Damping Ratios in Static Time History Analysis for Frame 6-3- P_a

Frame	ξ_{hyst}		
	SeismoStruct	OpenSees	Abaqus
6-3- P_a	12%	13%	13%

Figure 11 shows the final cycles obtained from two software programs that indicates acceptable agreement with the corresponding results.

After plotting the hysteresis loops, the required damping ratios from Eq. (1) were calculated. Table 8 shows the results of the static time history analysis for frame 6-3- P_a.

5.8 Comparison of Results for Frame 6-3- P_a

All the results obtained for frame 6-3- P_a from the different software types and analysis methods (sections 5.1, 5.3, 5.5, 5.6 and 5.7) have been plotted in Fig. 12. The horizontal axis shows the different software types and analysis methods based on Table 9, and the vertical axis shows the hysteretic damping ratios.

The average damping ratios obtained from the different kinds of software and analysis methods together with the DDBD method are also given in Fig. 12.

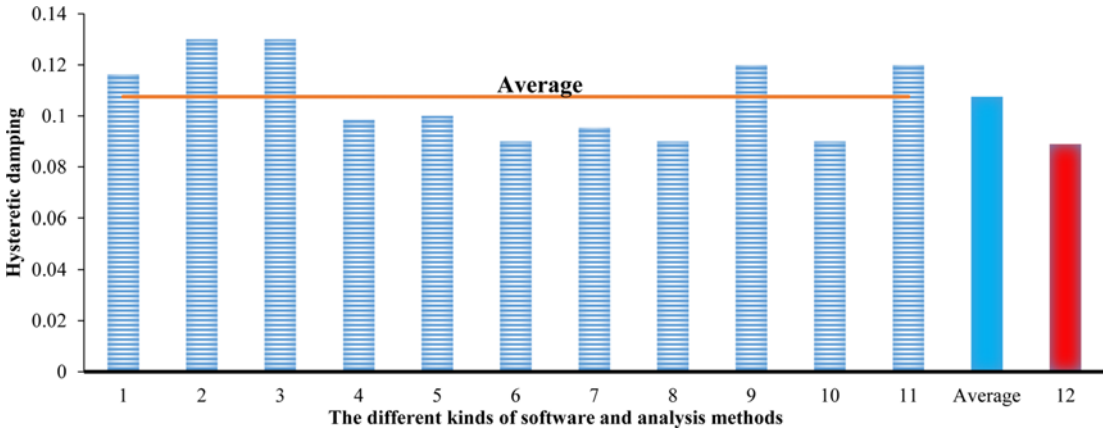

Fig. 12. Comparison of the Hysteretic Damping for Sample Frame 6-3- P_a in Different Kinds of Software and Analysis Methods

Table 9. Types of Software and Analysis Methods Used to Calculate Hysteretic Damping Ratio

Software type and analysis methods	Software	Analysis
1	SeismoStruct	Sinusoidal loading at initial period
2	Abaqus	
3	OpenSees	
4	SeismoStruct	Sinusoidal loading at equivalent period
5	Abaqus	
6	OpenSees	
7	SeismoStruct	Static Time History
8	Abaqus	
9	OpenSees	
10	SAP2000	Pushover in accordance with FEMA 440
11	SeismoSignal	Structural analysis of SDOF
12	Matlab	DDBD Method

6. Evaluation of Results of All Frames

The average values of the damping ratios obtained from the different kinds of software and the DDBD method for all frames are shown in Fig. 13.

Figure 13 indicates that the damping ratio is not very sensitive to changes in the number of spans, but as expected, increasing the height of the building, which is synonymous with increasing the number of beams and columns, slightly increased hysteretic damping. For instance, the damping ratio of a 3-story frame is about 9%, but, for a 15-story frame, this value increases to 14%. In DDBD method, these values are 9% and 10%, respectively. This emphasizes the necessity of correcting the equivalent damping formula (Eq. (17)) to provide a more accurate results.

The values of the damping ratios obtained from the different kinds of software and methods versus the relevant ductility

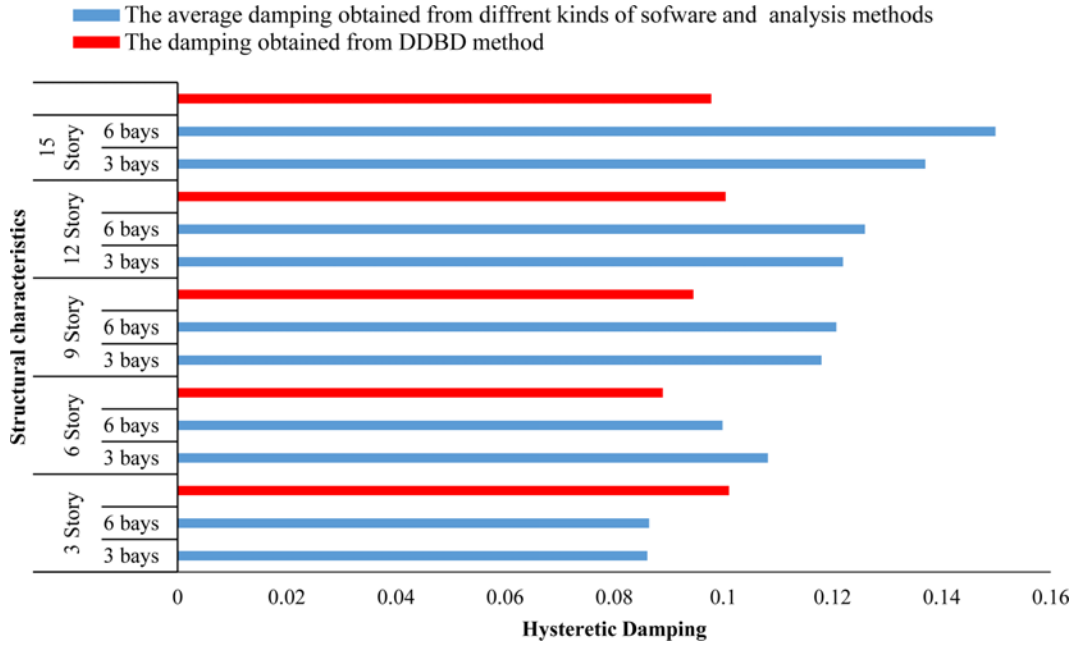

Fig. 13. Comparison of Average Damping Values Calculated using Different Methods and DDBD Method

values are plotted in Fig. 14.

After filtering the results obtained from Fig. 14 and fitting the results, the present study proposes Eq. (3) (ductility-dependent formulae) as the best formula for the ductile range of structures (Fig. 15).

$$\xi_{hyst} = 0.04e^{0.5\mu_\Delta} \tag{3}$$

The use of smaller damping values in the displacement-period spectral curves, (Fig. 1(d)), results in a shorter estimated period, which leads to a larger equivalent stiffness and a greater base shear. In other words, current underestimation of damping values for steel moment-resisting frames in the DDBD method yields in higher safety factors and much stronger structures. The prediction of a relation for damping ratio of these frames requires further analysis that focuses specifically on that range.

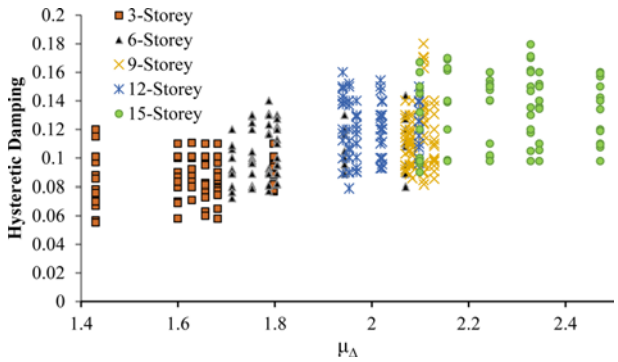

Fig. 14. Hysteretic Damping Based on the Ductility for Studied Frames

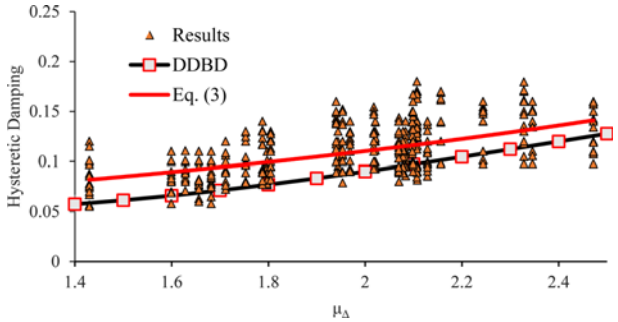

Fig. 15. Comparison of Hysteretic Damping Obtained by Eq. (3) and DDBD Method

Figure 16 shows the hysteretic damping ratio versus the initial period (T_i) and equivalent period (T_{eq}) for the studied frames.

Using two equations found in Fig. 16 the relationship between the hysteretic damping ratio and the equivalent-to-initial period ratio ($\frac{T_{eq}}{T_i}$) is proposed in the form of Eq. (4) (period-dependent formula).

$$\xi_{hyst} = \frac{0.104 - 0.065\left(\frac{T_{eq}}{T_i}\right)}{1.48 - \left(\frac{T_{eq}}{T_i}\right)} \tag{4}$$

In addition, Eq. (5) relates the equivalent-to-initial period ratio to ductility in accordance with ATC-40:

$$\frac{T_{eq}}{T_i} = \sqrt{\frac{\mu_\Delta}{1 + r_\Delta \mu_\Delta - r_\Delta}} \tag{5}$$

where r_Δ is the post-yield slope previously shown in Fig. 1(b).

Using Eq. (4) and Eq. (5), the relationship between the hysteretic damping ratio and the ductility can be found which is shown in Fig. 17 together with Eq. (3) and DDBD equation.

Figure 17 shows that the differences between the results of

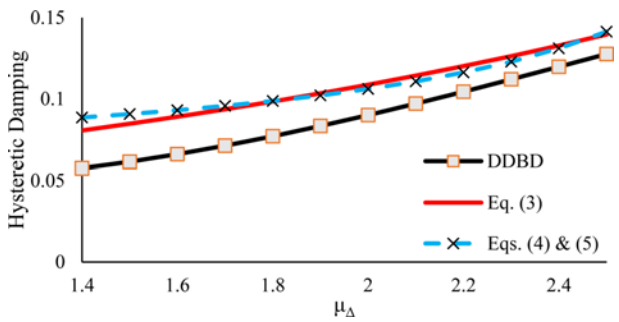

Fig. 17. Comparison of Hysteretic Damping Ratios in DDBD Method and Proposed Formulas for the Desired Ductility

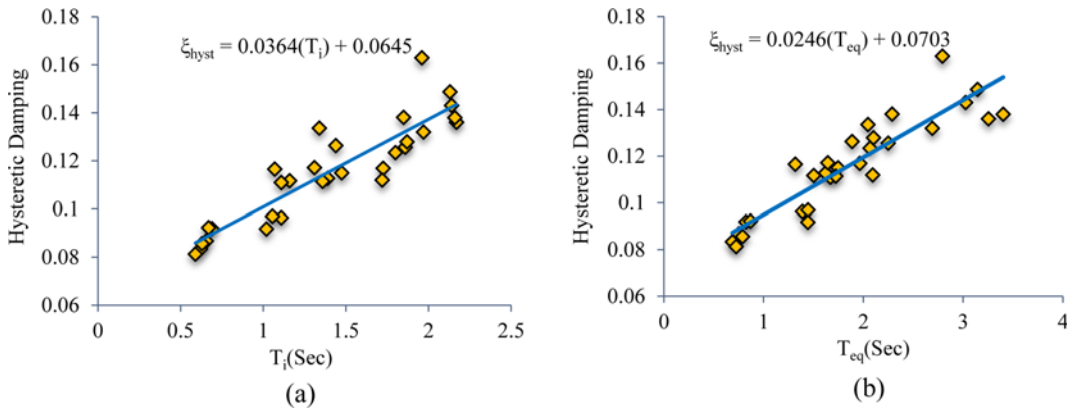

Fig. 16. Hysteretic Damping Based on: (a) Initial Period, (b) Equivalent Period

analysis and formulas proposed by DDBD method are more significant in lower ductility values and less pronounced for higher values of ductility.

7. Conclusions

This paper proposes a reliable relation for hysteretic damping of steel moment-resisting frames at the life safety performance level for use in the DDBD method. The hysteretic damping values for different SMRFs under various loading conditions were examined and compared with those of DBDD method. The remarkable results are summarized below:

1. An exponential damping-ductility formula is presented for SMRFs for ductility values up to 2.5.
2. Two fractional formulas are presented that correlate damping to the initial and equivalent periods of steel moment-resisting frames.
3. The consistency between period-dependent and ductility-dependent formulas confirms the accuracy of results.
4. There is a significant difference between the equivalent damping ratios estimated herein and those estimated by the formula presented in the DBDD method. The results show that the damping values of DBDD method have been underestimated.

References

AISC (2010). *Specification for Structural Steel Buildings*, American Institute of Steel Construction AISC 360-10, Inc., Chicago, IL, USA.

ASCE (2010). *Minimum Design Loads for Buildings and Other Structures,* American Society of Civil Engineers ASCE 7–10, Reston, Virginia.

ATC (1996). *Seismic Evaluation and Retrofit of Concrete Buildings*, ATC-40, Applied Technology Council, Redwood City, California, Vol. 1, USA.

Blandon, C. A. and Priestley, M. J. N. (2005). "Equivalent viscous damping equations for direct displacement based design." *Journal of earthquake Engineering*, Vol. 9, No. 2, pp. 257-278, DOI: 10.1142/S1363246905002390.

Boulaouad, A. and Amour, A. (2011). "A displacement-based seismic design for reinforced concrete structures." *KSCE Journal of Civil Engineering*, Vol. 15, No. 3, pp. 507-516, DOI: 10.1007/s12205-011-1009-z.

Calvi, G. M. and Sullivan, T. J. (2009). *A Model Code for the Displacement-based Seismic Design of Structures*: DBD09 Draft Subject to Public Enquiry, ISBN: 978-88-6198-038-9.

Cecilia, I., Timothy, N. and Sullivan, J. (2015). "Applicability of the direct displacement-based design method to steel moment resisting frames with setbacks." *Bull Earthquake Engineering,* Vol. 13, pp. 3841-3870, DOI: 10.1007/s10518-015-9787-1.

Chopra, A. K. (2013). *Dynamics of structures theory and applications to earthquake engineering*, 4th edition, Lebanon, Indiana, U.S.A.: Prentice Hall, ISBN 10: 0-13-285803-7.

Dimopoulos, A. I., Bazeos, N., and Beskos., D. E. (2012). "Seismic yield displacements of plane moment resisting and x-braced steel frames." *Soil Dynamics and Earthquake Engineering*, Vol. 41, pp. -140, DOI: 10.1016/ j.soildyn.2012.05.002.

Dwairi, H. M. (2004). *Equivalent Damping in Support of Direct Displacement-Based Design and Applications to Multi-span Bridges*, Ph.D. Thesis, North Carolina State University, Raleigh, NC.

Dwairi., H. M., Kowalsky., M. J., and Nau., J. M. (2007). "Equivalent damping in support of direct displacement-based design. " *Journal of Earthquake Engineering*, Vol. 11, No. 4, pp. 512-530, DOI: 10.1080/136324606010 33884.

Esmaeilabadi, R. (2016). *Improving the parameters of directly displacement-based design in steel moment resisting frames*, Ph.D. Thesis, Science and Research Branch, Islamic Azad University.Tehran,Iran.

FEMA356 (2000). *Prestandard and commentary for the seismic rehabilitation of buildings*, FEMA356, in rehabilitation requirements, Federal Emergency Management Agency, Washington, DC, USA.

FEMA440 (2005). *Improvement of nonlinear static seismic analysis procedures,* Federal Emergency Management Agency, Washington DC, USA.

Gasparini, D. and Vanmarcke, E. H. (1976). "SIMQKE—a program for artificial motion generation, user's manual and documentation." *Massachusetts Institute of Technology*, Massachusetts, USA

INBCSD (2013). *Iranian National Building Codes for Structural Design. Part 10: Design of steel buildings*, Tehran, Iran.

Nievas, C. I. and Sullivan, T. J. (2015). "Applicability of the direct displacement-based design method to steel moment resisting frames with setbacks." *Bulletin of Earthquake Engineering*, Vol. 13, No. 12, pp. 3841-3870, DOI: 10.1007/s12205-011-1009-z.

Powell, G. H. and Emeritus (2013). "Static pushover methods - explanation, comparison and implementation." *Retrieved from https://wiki.csiamerica.com*

Priestley, M. J. N. (1993). "Myths and fallacies in earthquake engineering – conflicts between design and reality." *Bulletin of the New Zealand National Society for Earthquake Engineering*, Vol. 26, No. 3, pp. 329-341.

Priestley, M. J. N., Calvi, G. M., and Kowalsky, M. J. (2007). *Displacement-based Seismic Design of Structures*. IUSS Press, Pavia. ISBN: 978-88-6198-000-6.

SeismosSignal ver 5.1.0 (2015). *A Program Process Strong-montion data*, URL: http://www.seismosoft.com/ SeismoSignal/.

Shibata, A. and Sozen, M. A. (1976). "Substitute structure method for seismic design in R/C." *ASCE, Journal of Structure Engineering*, Vol. 102, No. 1, pp. 1-18.

Standard No. 2800 (2014). *Iranian Code of Practice for Seismic Resistant Design of Buildings*, Standard No. 2800, 4th edition, BHRC Publication No. S-253, Iran, Tehran.

Sullivan, T. J., Priestley, M. J. N., and Calvi, G. M. (2012). *A Model Code for the Displacement-Based Seismic Design of Structures (DBD12)*, ISBN: 978-88-6198-072-3.

Wijesundara, K. K., Nascimbene, R., and Sullivan T. J. (2011). "Equivalent viscous damping for steel concentrically braced frame structures." *Bulletin of Earthquake Engineering*, Vol. 9, No. 5, pp. 1535-1558, DOI: DOI 10.1007/ s10518-011-9272-4.

Appendix

A. Determining the Design Displacement for the Stories (Δ_i)

The displacement ratio for each story is e $^{\Delta_i}$ stimated based on a displacement profile or a shape function. The shape functions in Eqs. (6) and (7) are used for moment frames:

$$\varphi_i = \frac{4}{3}\left(\frac{H_i}{H_n}\right)\left(1-\frac{H_i}{4H_n}\right) \quad (\text{for } n_s \geq 46) \tag{6}$$

$$\varphi_i = \left(\frac{H_i}{H_n}\right) \quad \text{for } n_s < 4 \tag{7}$$

where φ_i (i = 1, 2, …, n_s) is the displacement profile and is obtained based on the first inelastic mode of the structure, n_s is the number of stories, H_i is the height of the ith story, and H_n is the roof level height.

The design displacement at each story level can be obtained from Eq. (8) as:

$$\Delta_i = \varphi_i\left(\frac{\Delta_c}{\varphi_c}\right) \tag{8}$$

where φ_c is the displacement profile of the critical story (first story) and Δ_c is the design displacement of the critical story.

Using Eq. (8) and fundamental structural dynamics equations, the design displacement of the structure at the desired performance level can be obtained in Eq. (9) as:

$$\Delta_i = \omega_\theta \theta_c H_i \left(\frac{4H_n - H_i}{4H_n - H_1}\right) \tag{9}$$

where Δ_i is the design displacement of story i, θ_c is the code design drift (2.0% for the life safety limit state in this study) and ω_θ is the higher mode reduction factor obtained from Fig. 18 based on the number of stories.

B. Obtaining the Target Displacement (Δ_d)

The target displacement is obtained using Eq. (10) as:

$$\Delta_d = \frac{\sum_{i=1}^{n} m_i \Delta_i^2}{\sum_{i=1}^{n} m_i \Delta_i} \tag{10}$$

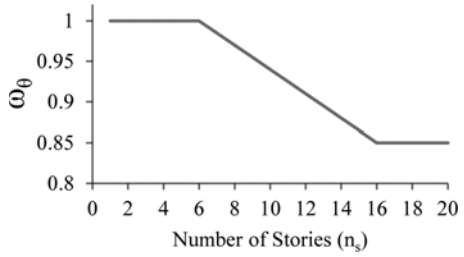

Fig. 18.Variations in ω_θ, According to the Number of Stories (Nievas *et al.*, 2015)

where m_i is the mass of the ith story.

C. Equivalent Mass and Height (M_{eq}, h_{eq})

The characteristics of the substitute structure, including the equivalent mass and height, are obtained from Eqs. (11) and (12):

$$M_{eq} = \frac{\sum_{i=1}^{n} m_i \Delta_i}{\Delta_d} \tag{11}$$

$$h_{eq} = \frac{\sum_{i=1}^{n} m_i \Delta_i H_i}{\sum_{i=1}^{n} m_i \Delta_i} \tag{12}$$

D. Calculating the Design Displacement Ductility (μ_Δ)

Equation (13) is used to calculate μ_Δ as:

$$\mu_\Delta = \frac{\Delta_d}{\Delta_y} \tag{13}$$

where Δ_y is the yield displacement. Because the bay width will normally exceed story height and column curvature will typically be less than beam curvature as a consequence of capacity design procedures, beam flexibility is likely to be the major contributor to deformation (Priestley *et al*., 2007); hence, yield rotation θ_y can be obtained using Eq. (14) and Δ_y can be estimated from Eq. (15) as:

$$\theta_y = 0.65\varepsilon_y \frac{L_b}{H_b} \tag{14}$$

$$\Delta_y = \theta_y \times h_{eq} \tag{15}$$

where L_b is the span length of the beams, H_b is the section height of the beams and ε_y is the yield strain.

E. Calculation of equivalent viscous damping ratio (ξ_{eq})

The equivalent damping ratio for the substitute structure can be obtained from Eqs. (16) and (17) as:

$$\zeta_{eq} = \xi_v + \xi_{hyst} \tag{16}$$

$$\zeta_{eq} = 0.05 + C_v\left(\frac{\mu_\Delta - 1}{\mu_\Delta \pi}\right) \tag{17}$$

where ξ_v is the elastic damping in the elastic zone which is usually assumed to be 5%. ξ_{hyst} is the hysteretic damping. Cv coefficient for steel moment-resisting frames is 0.577 (Sullivan *et al*., 2012). Eq. (17) is an empirical relation and was obtained through various analyses in the nonlinear method. The purpose of this study is to control and modify it if needed.

F. Calculation of Equivalent Period of Substitute Structure (T_{eq})

Using target displacement and the reduced elastic displacement spectrum (with different damping values), the equivalent period can be obtained as shown in Fig. 1(d).

G. Calculation of Equivalent Stiffness (K_{eq}) and Base Shear (F)

The equivalent stiffness and base shear can be obtained using Eqs. (18) and (19) (Boulaouad *et al*., 2011) as:

$$k_{eq} = 4\pi^2\left(\frac{M_{eq}}{T_{eq}^2}\right) \tag{18}$$

$$F = k_{eq} \times \Delta_d \tag{19}$$